## Title

Mouse HORMAD1 Is a Meiosis I Checkpoint Protein That Modulates DNA Double-Strand Break Repair During Female Meiosis1



## Journal

Biology of Reproduction, 89(2)

## ISSN

0006-3363

## Authors

Shin, Yong-Hyun
McGuire, Megan M
Rajkovic, Aleksandar

## Publication Date

2013-08-01

## DOI

10.1095/biolreprod.112.106773

Peer reviewed

BIOLOGY OF REPRODUCTION (2013) **89**(2):29, 1–12
Published online before print 12 June 2013.
DOI 10.1095/biolreprod.112.106773

# Mouse HORMAD1 Is a Meiosis I Checkpoint Protein That Modulates DNA Double-Strand Break Repair During Female Meiosis[1]

**Yong-Hyun Shin,[3] Megan M. McGuire,[3] and Aleksandar Rajkovic[2,3,4,5]**

[3]*Magee-Womens Research Institute, Department of Obstetrics, Gynecology, and Reproductive Sciences, University of Pittsburgh, Pittsburgh, Pennsylvania*
[4]*Department of Human Genetics, University of Pittsburgh, Pittsburgh, Pennsylvania*
[5]*Department of Pathology, University of Pittsburgh, Pittsburgh, Pennsylvania*

## ABSTRACT

**Oocytes in embryonic ovaries enter meiosis I and arrest in the diplonema stage. Perturbations in meiosis I, such as abnormal double-strand break (DSB) formation and repair, adversely affect oocyte survival. We previously discovered that HORMAD1 is a critical component of the synaptonemal complex but not essential for oocyte survival. No significant differences were observed in the number of primordial, primary, secondary, and developing follicles between wild-type and *Hormad1*$^{-/-}$ newborn, 8-day, and 80-day ovaries. Meiosis I progression in *Hormad1*$^{-/-}$ embryonic ovaries was normal through the zygotene stage and in oocytes arrested in diplonema; however, we did not visualize oocytes with completely synapsed chromosomes. We investigated effects of HORMAD1 deficiency on the kinetics of DNA DSB formation and repair in the mouse ovary. We irradiated Embryonic Day 16.5 wild-type and *Hormad1*$^{-/-}$ ovaries and monitored DSB repair using gamma-H2AX, RAD51, and DMC1 immunofluorescence. Our results showed a significant drop in unrepaired DSBs in the irradiated *Hormad1*$^{-/-}$ zygotene oocytes as compared to the wild-type oocytes. Moreover, *Hormad1* deficiency rescued *Dmc1*$^{-/-}$ oocytes. These results indicate that *Hormad1* deficiency promotes DMC1-independent DSB repairs, which in turn helps asynaptic *Hormad1*$^{-/-}$ oocytes resist perinatal loss.**

*double-strand break repair, HORMAD1, meiosis I, oocyte, ovary*

## INTRODUCTION

Oocytes in mice enter meiosis circa Embryonic Day (E) 13.5 and arrest in diplonema of meiosis I. The oocytes in the embryonic mouse gonad are physically located in germ cell clusters (also known as cysts), where they are connected via intercellular bridges. Oocyte clusters break down shortly after birth to form primordial follicles, where individual oocytes become enveloped with a single layer of flat granulosa cells. Thus formed, primordial follicles are recruited regularly to grow and form a mature egg. More than half of oocytes are naturally lost during the primordial follicle formation [1]. Abnormal meiosis can accelerate oocyte loss and diminish the primordial follicle pool [2–7]. Synaptonemal complex proteins (*Sycp1*, *Sycp2*, and *Sycp3*) are important prosurvival factors, and their deficiency accelerates germ cell loss [5–11]. DMC1, a meiosis-specific recombinase, is important in oocyte survival, and its deficiency leads to the accumulation of the extensively resected double-strand breaks (DSBs) and to massive oocyte loss [3]. ATM is a kinase that controls DSB formation [4, 12], and its deficiency also leads to massive oocyte loss. Unrepaired DSBs are associated with genomic instability and trigger apoptosis with subsequent oocyte death [13]. SPO11 is a *trans*-esterase that initiates DSB formation [14]. Mice deficient in *Spo11*, and therefore unable to generate DSBs, have been used to determine the importance of DSBs in oocyte loss. Oocyte loss in *Atm* and *Dmc1* mutants is partially rescued in *Spo11*-deficient mice, presumably because DSBs do not form [14, 15]. However, DSBs are not the only determinants of oocyte loss, because *Spo11* mutants themselves show accelerated loss of oocytes [16]. These experiments suggest that DSB-dependent as well as DSB-independent mechanisms trigger oocyte loss when recombination defects occur.

Our group as well as others have recently discovered that meiosis-specific HORMA domain-containing 1 (HORMAD1) likely is the mammalian counterpart of yeast Hop1 and that *Hormad1* deficiency disrupts mammalian synaptonemal complex formation, meiotic recombination, and chromosome segregation [9, 17–21]. Proteins with HORMA domain are critical components of the axial elements [22], and in nonmammalian organisms, several meiosis-specific HORMA proteins, such as Hop1 [23] and Red1 [24] in yeast, Him-3 [25, 26] in nematodes, and Asy1 [27] in plants, are critical for meiosis. In yeast, plants, and nematodes, HORMA domain proteins are critical components of the synaptonemal complex and essential for meiosis I [9, 19, 21]. Mouse and yeast HORMA domains in HORMAD1 and Hop1 share 28% amino acid identity, and HORMAD1 likely is the mammalian homologue of Hop1. Hop1 in yeast appears to bind near or at the sites of DSB formation and modulates the initial DSB cleavage [28]. Hop1 mutants in yeast have a reduced number of DSBs [20], and Hop1 may participate in recruiting DMC1, RAD51, and other proteins that are required for DNA repair during meiotic synapsis and recombination [19, 20]. Phosphorylation of Hop1 by Mec1/Tel1 yeast kinases is important for interhomologue recombination and prevents DMC1-independent repair of meiotic DSBs [21]. In mammals, HORMAD1 deficiency disrupts synaptonemal complex formation; however, folliculogenesis is apparently normal, with no gross evidence of accelerated oocyte loss [9, 19, 21]. These results indicate that HORMAD1 is an important checkpoint protein in female meiosis. Moreover, *Hormad1* deficiency rescued accelerated loss of oocytes in *Spo11* mutants, indicating that HORMAD1 is an important contributor to

[1]Supported in part by the National Institutes of Health grant HD054829 to A.R.
[2]Correspondence: Aleksandar Rajkovic, Magee-Womens Research Institute, Department of Obstetrics, Gynecology, and Reproductive Sciences, University of Pittsburgh, 204 Craft Ave., Pittsburgh, PA 15213. E-mail: rajkovic@upmc.edu

Received: 7 December 2012.
First decision: 4 January 2013.
Accepted: 29 May 2013.

eISSN: 1529-7268 http://www.biolreprod.org
ISSN: 0006-3363

DSB-independent mechanisms of asynaptic surveillance [19, 21]. It is unknown whether HORMAD1 regulates DSB formation and how DSB formation and repair in *Hormad1*-deficient ovaries contributes to oocyte survival. To further understand how *Hormad1* deficiency prevents an excessive loss of oocytes, we carefully assessed meiosis I in female meiocytes by studying the kinetics of DSB repair in *Hormad1*-deficient animals and the effects of *Hormad1* deficiency on *Dmc1* mutants. Our results are consistent with the interpretation that HORMAD1 regulates DSB repair by inhibiting DMC1-independent DSB repair mechanisms and that *Hormad1* deficiency promotes DSB repair. HORMAD1 therefore acts as a pachytene-stage checkpoint protein in part by modulating DSB formation in female meiocytes.

## MATERIALS AND METHODS

### Animal Breeding

All mouse experiments were carried out on the 129S7/SvEvBrd × C57BL/6 hybrid background. All experimental and surgical procedures complied with the Guide for the Care and Use of Laboratory Animals and were approved by the Institutional Animal Care and Use Committee at the University of Pittsburgh. *Hormad1*$^{+/-}$ mice were as previously described [9]. *Atm*$^{+/-}$ and *Dmc1*$^{+/-}$ mice were purchased from The Jackson Laboratory [2, 29].

### Histology, Immunostaining, and Quantification

Ovaries were fixed in 10% buffered formalin (Sigma-Aldrich). Fixed tissues were embedded in paraffin, serially sectioned (section thickness, 5 μm), and stained with hematoxylin (Sigma-Aldrich) and periodic acid-Schiff. At least five pairs of testes and ovaries from each genotype were subjected to gross and microscopic analyses at each time point. Germ cell cysts and primordial, primary, and secondary follicles were defined as described previously [10]. Wild-type and mutant oocytes were stained concurrently with the same mixture of antibodies. Anti-NOBOX and anti-LHX8 antibody was used to identify oocytes [8, 10].

### Quantification of the Immunofluorescence Signal

Wild-type and mutant oocytes were stained concurrently with the same mixture of antibodies. For multiphoton excitation laser-scanning microscopy (Olympus Fluoview FV1000MPE, Olympus), ovaries were fixed in 4% paraformaldehyde and incubated with the Sca*l*e A2 reagent for 2 wk [30]. Oocytes were labeled with anti-LHX8 antibody, and multiphoton excitation laser-scanning microscopy was used to detect immunofluorescence. Images were taken at 2-μm steps. In each experiment, when comparing wild-type and mutants, imaging of the ovaries was performed on the same day with the same microscope and camera settings. PerkinElmer Volocity 6.1 software was used to control for changes in illumination during the course of imaging and measurement of the immunofluorescence. We measured total fluorescence of γH2AX in identically sized rectangles that were placed over the cell boundaries as previously described [9]. Fifty individual oocytes were subjected to immunofluorescence analysis.

### Ovary In Vitro Culture and Irradiation

Intact ovaries from E15.5 mice were cultured for 1 day as previously described [31]. Ovaries were isolated from E15.5 mice, and surrounding tissue, including the ovarian bursa, was removed. The ovaries were placed on Millicell-PC membrane inserts (pore size, 3.0 μm; diameter, 30 mm; Millipore Corp.) with media filling only the lower chamber. Each ovary was placed on the membrane with a single drop of medium, and eight ovaries were placed on each membrane. The medium was removed from the lower chamber until only a thin film covered the ovaries. The medium for organ culture was Waymouth MB752 (Life Technologies) supplemented with 0.23 mM pyruvic acid (Sigma-Aldrich), 10 μg/ml of streptomycin sulfate (Sigma-Aldrich), 75 μg/ml of penicillin G (Sigma-Aldrich), and 10% fetal bovine serum (Thermo Fisher). Organ cultures were maintained for 1 day in a 37°C incubator thoroughly infused with a gas mixture of 5% $CO_2$ and balanced air. The next day, select wild-type and *Hormad1*$^{-/-}$ ovaries were subjected to irradiation via a Nordion Gamma Cell 1000 Irradiator. Ovaries received 2 Gy (1 Gy = 100 rads) at a dose of 120 rads/min. The irradiated ovaries were collected at 1 and 8 h after treatment and immediately processed to prepare chromosome spreads as previously described [9].

## RESULTS

### Hormad1 *Deficiency Does Not Accelerate Ovarian Follicle Loss*

Our previous gross assessment of the ovaries found no significant differences between the number of various follicles in wild-type and *Hormad1*-deficient animals [9]. We carefully reassessed these numbers by the well-accepted histomorphometric analysis [8] as well as by fluorescence imaging of the whole ovary [30]. Histomorphometric assessment of the newborn wild-type and *Hormad1*$^{-/-}$ ovaries identified 1333.4 ± 238.0 (mean ± SEM throughout) and 1730.3 ± 100.3 primordial follicles, respectively, and the counts did not differ significantly ($P > 0.1$) (Supplemental Fig. S1, A–C, available online at www.biolreprod.org). At 8 days of age, 1128 ± 139 (n = 5) and 1383 ± 155.2 (n = 5) primordial follicles, 71.5 ± 2.4 and 73.8 ± 3.3 primary follicles, and 95.3 ± 4.7 and 115 ± 4.4 secondary follicles were counted in wild-type and *Hormad1*$^{-/-}$ ovaries, respectively, and these counts did not differ significantly ($P > 0.1$) (Supplemental Fig. S1, D–F). Furthermore, in 80-day-old ovaries, we counted 619 ± 238.5 and 704 ± 147.0 primordial follicles, 45.7 ± 5.5 and 44.3 ± 7.2 primary follicles, 61.5 ± 9.2 and 48.8 ± 6.6 secondary follicles, 27.0 ± 10.2 and 26.6 ± 6.5 preantral follicles, and 10.3 ± 3.9 and 11.5 ± 4.1 antral follicles in wild-type (n = 5) and *Hormad1*$^{-/-}$ (n = 5) ovaries, respectively, and these counts did not differ significantly ($P > 0.1$) (Supplemental Fig. S1, G–I).

Serial sectioning and histomorphometric oocyte counting is prone to errors due to many confounders [1, 32]. We therefore used multiphoton excitation laser-scanning microscopy on whole-mount ovaries that were treated with Sca*l*eA2 reagent [30] as an alternative way to compare germ cell numbers in *Hormad1*$^{-/-}$ and wild-type ovaries. We quantitated immunofluorescence of LHX8, an oocyte-specific marker that labels oocyte nuclei. We did not find significant difference in the LHX8 immunofluorescence between wild-type and *Hormad1*$^{-/-}$ ovaries (Supplemental Fig. S1, J–L). The results of our analyses indicate that *Hormad1* deficiency had no effect on the naturally occurring perinatal oocyte loss. Interestingly, a trend toward a greater number of primordial oocytes was observed in *Hormad1*-deficient ovaries, but this trend was not statistically significant.

### *Meiosis I in* Hormad1*-Deficient Oocytes*

We also investigated the molecular anatomy of *Hormad1*$^{-/-}$ female meiocytes to better understand events preceding massive perinatal oocyte loss. Meiosis in mouse ovaries commences circa E13.5 and arrests in the diplotene stage before birth. By E16.5, most oocytes show zygotene and pachytene stages of meiosis, whereas at E18.5, pachytene and diplotene stages predominate. The substages of meiosis I prophase are defined by chromosome configurations and structures: pairing, which occurs during the leptotene and zygotene stages; synapsis, which is completed at the onset of the pachytene stage; and desynapsis, which occurs during the diplotene stage [33]. Recombination is initiated by DSBs, and these breaks are repaired by either crossover or noncrossover events [16, 34, 35].

We compared the E16.5 and E18.5 wild-type and *Hormad1*$^{-/-}$ ovaries for meiosis-stage progression using the centromere specific anti-CREST antibody and anti-SYCP2

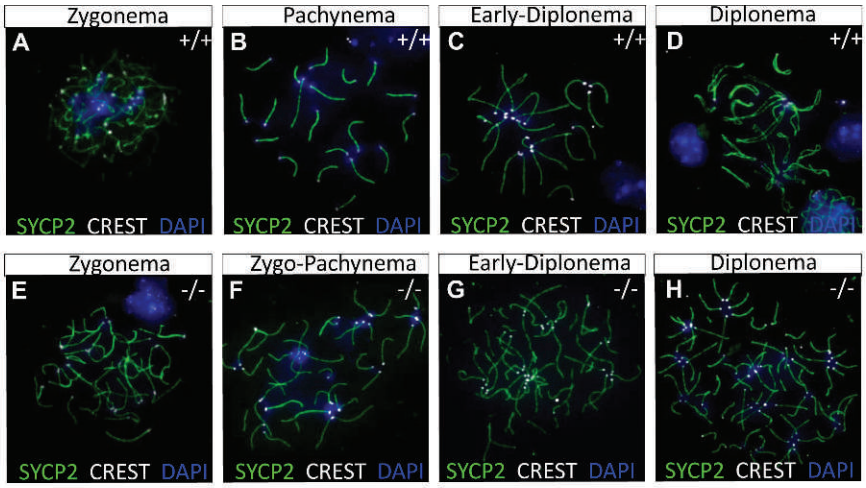


| | | | | | |
|---|---|---|---|---|---|
| E16.5 | WT | 22.62% | 58.93% | 2.38% | 16.07% |
| | KO | 34.15% | 23.17% | 30.49% | 12.20% |
| E18.5 | WT | 6.56% | 35.25% | 9.02% | 49.18% |
| | KO | 17.56% | 16.03% | 21.37% | 45.04% |
| NB | WT | 3.37% | 4.49% | 14.61% | 77.53% |
| | KO | 1.74% | 5.23% | 5.23% | 87.79% |

FIG. 1. Meiosis I progression in *Hormad1*$^{-/-}$ ovaries. Chromosomal spreads were performed on meiocytes from E16.5, E18.5, and newborn (NB) wild-type (+/+) and *Hormad1*$^{-/-}$ (–/–) ovaries. Representative spreads are shown in **A**–**D** for wild-type ovaries and **E**–**H** for *Hormad1*$^{-/-}$ ovaries. Immunofluorescence staining with anti-SYCP2 (green) and CREST (white) was used to label axial lateral elements and centromeres, respectively. The proportion of various meiotic stages observed at various ages in either wild-type (WT) or *Hormad1*$^{-/-}$ (KO) ovaries is shown in a table below the figure panels. We failed to find pachynema oocytes in *Hormad1*$^{-/-}$ embryonic ovaries. Incompletely synapsed zygotene had 40 CREST foci (in wild type ovaries; 40-30 foci in *Hormad1*$^{-/-}$ ovaries). *Hormad1*$^{-/-}$ zygopachynema show incompletely synapsed chromosomes with 20–30 CREST foci, whereas wild-type pachynema are synapsed (by SYCP2 staining) with 20 CREST foci. Wild-type and *Hormad1*$^{-/-}$ diplotene contain D-loop structures. DNA was stained with 4′,6-diamidino-2-phenylindole (blue). Original magnification ×100.

antibody [18] (Fig. 1). In the wild type, zygonema is characterized by unsynapsed axes and 40 CREST foci, whereas pachynema is characterized by synapsed chromosomes with 20 CREST foci and diplonema is characterized by desynapsed axes with a D-loop structure. We did not find a significant difference in the number of zygotene-stage cells between the wild-type and *Hormad1*$^{-/-}$ ovaries (Fig. 1, A and E). At E16.5, 35% fewer zygopachytene oocytes and 18% more early diplotene oocytes that had the D-loop were observed in the *Hormad1*$^{-/-}$ ovaries as compared to the wild-type ovaries ($P < 0.01$). At E18.5, 19% fewer zygopachytene-like stage and 12% more early diplotene oocytes were observed in the *Hormad1*$^{-/-}$ ovaries (Fig. 1, B and F) ($P < 0.01$). We did not identify oocytes with completely synapsed chromosomes in E16.5 or E18.5 *Hormad1*$^{-/-}$ ovaries, versus 59% and 35% pachynema oocytes observed in E16.5 and E18.5 wild-type ovaries, respectively (Fig. 1, B, C, F, and G). Amazingly, the number of diplonema oocytes did not significantly differ between the wild-type and *Hormad1*$^{-/-}$ ovaries (Fig. 1, D and F). Despite the lack of synapsed chromosomes, asynaptic oocytes are not eliminated in *Hormad1*-deficient ovaries, consistent with designating HORMAD1 as a pachytene checkpoint protein [19].

## Hormad1 *Deficiency Accelerates DSB Repair*

We previously showed that zygotene-stage *Hormad1*$^{-/-}$ oocytes exhibit a drastically reduced number of γH2AX foci, a marker for DSB formation [9, 19]. DMC1, RAD51, and RPA, all homologous recombination DSB repair proteins, were also reduced in *Hormad1*$^{-/-}$ ovaries [9]. We hypothesized that HORMAD1 modulates DSB formation, because unrepaired DSBs have been associated with accelerated oocyte loss [2–4]. We irradiated E16.5 wild-type and *Hormad1*$^{-/-}$ ovaries with 2 Gy of gamma radiation (Fig. 2A) and used γH2AX as a marker for DSB foci formation at various intervals following irradiation [36, 37]. Both wild-type and *Hormad1*$^{-/-}$ zygotene oocytes showed a greater than 2-fold increase in the γH2AX signal in ovaries exposed to 2 Gy for 1 h as compared to the nonirradiated ovaries (Fig. 2, Ba, Bb, Bd, Be, and C). Eight hours after radiation, wild-type zygotene oocytes retained almost 80% of the γH2AX signal, whereas only 46% of the γH2AX signal remained in the *Hormad1*$^{-/-}$ zygotene oocytes. The drop in γH2AX signal in the *Hormad1*$^{-/-}$ zygotene oocytes was statistically significant ($P < 0.01$), and the intensity of γH2AX signal in irradiated *Hormad1*$^{-/-}$ zygotene oocytes did not significantly differ from nonirradiated *Hormad1*$^{-/-}$ zygotene oocytes 8 h after irradiation or sham treatment (Fig. 2, Bc, Bf, and C). The rapid drop in γH2AX signal 8 h after irradiation in *Hormad1*$^{-/-}$ oocytes is consistent with activation of DSB repair pathways.

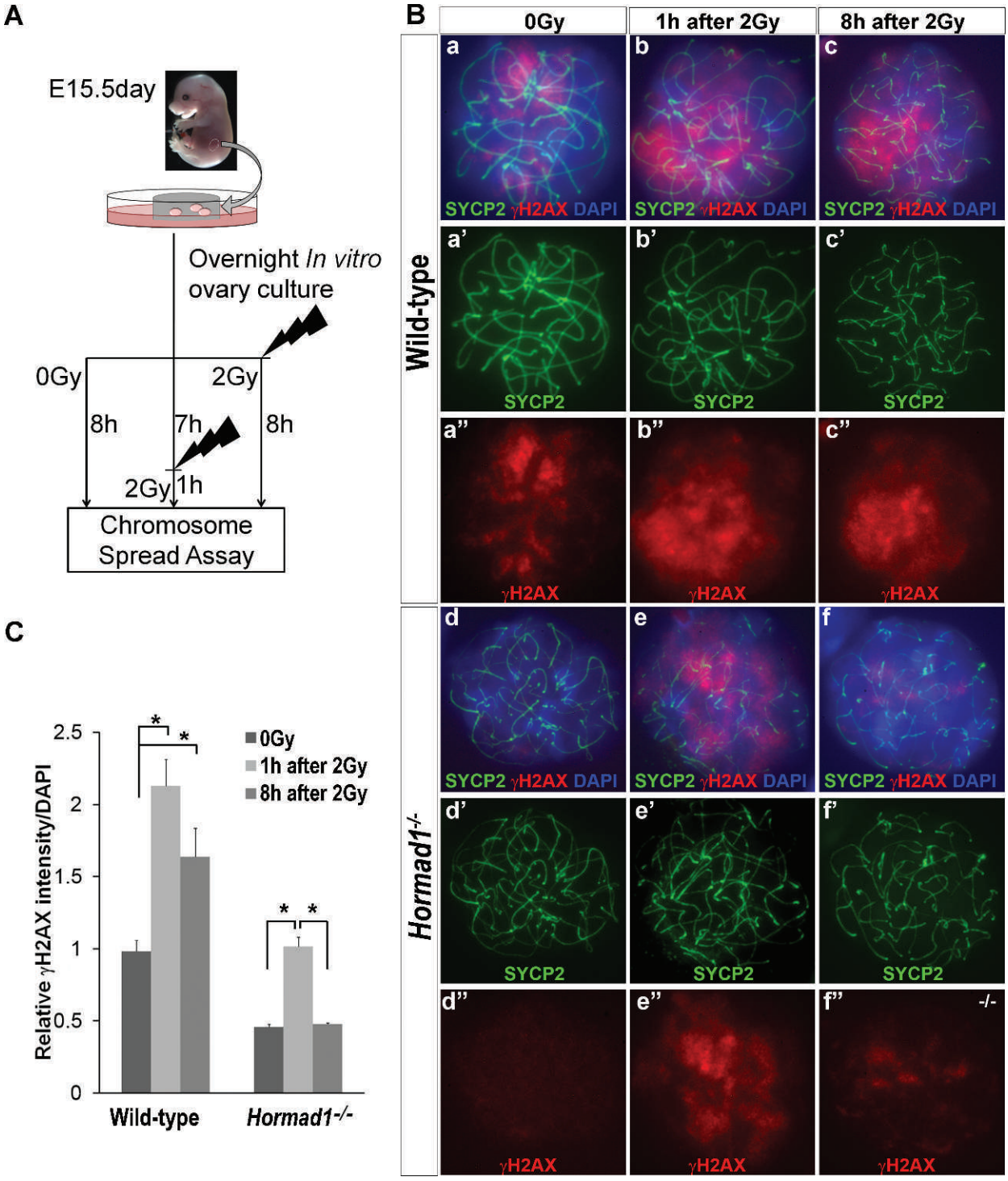


FIG. 2. *Hormad1* deficiency accelerates DSB repair. **A**) Diagram of the experimental design. The E15.5 wild-type and *Hormad1*$^{-/-}$ ovaries were harvested and cultured in Waymouth MB752 medium overnight while genotyping was performed. Cultured ovaries were exposed to 2 Gy of gamma rays. Chromosome spread assays were performed on irradiated wild-type and *Hormad1*$^{-/-}$ ovaries either 1 or 8 h after the exposure to gamma rays. Nonirradiated ovaries (0 Gy) were collected and analyzed after the same culture period as irradiated ovaries. **B**) Immunofluorescence with anti-SYCP2 (green) and anti-γH2AX (red) antibodies in wild-type (**a**–**c**) and *Hormad1*$^{-/-}$ zygotene oocytes (**d**–**f**) at various time points following irradiation. DNA was stained with 4′,6-diamidino-2-phenylindole (DAPI; blue). Original magnification ×100. **C**) Relative γH2AX intensity, normalized against DAPI signal, for indicated genotype and postexposure time points. Error bars represent the SEM. Student *t*-test was used to calculate *P*-values (*$P < 0.01$).

### Hormad1 *Deficiency Accelerates DMC1-Independent DSB Repair Pathways*

We investigated DMC1 and RAD51 foci formation in irradiated E16.5 wild-type and *Hormad1*$^{-/-}$ ovaries to determine which DSB repair pathway was activated in *Hormad1*$^{-/-}$ ovaries. DMC1 is a meiosis-specific recombinase important for DSB repair and interhomologue recombination. In the wild-type zygotene oocytes, the meiosis-specific recombinase DMC1 foci formation increased by 46% at 1 h

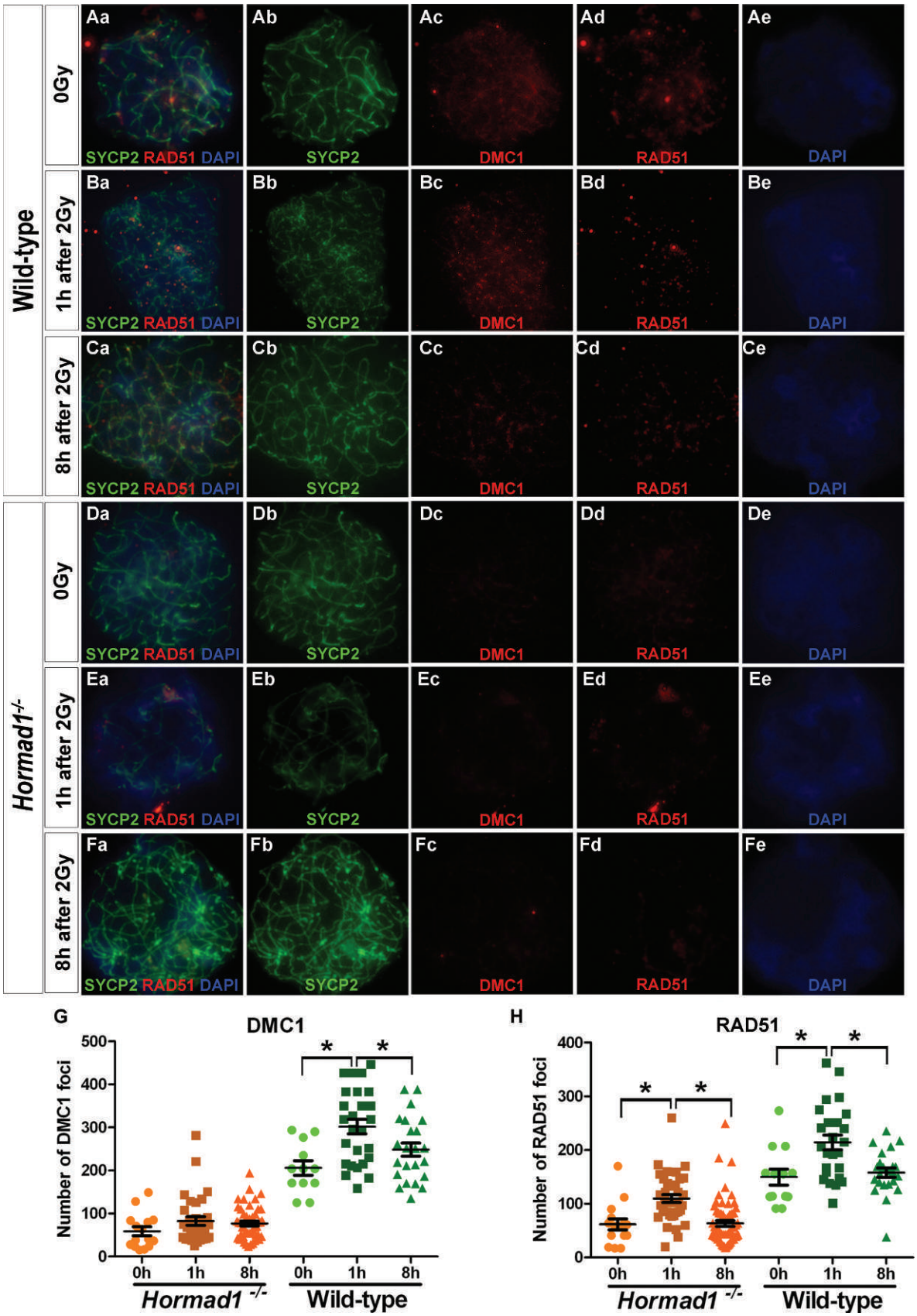


FIG. 3. *Hormad1* deficiency leads to DSB repair by DMC1-independent manner. The E15.5 wild-type and *Hormad1*$^{-/-}$ ovaries were cultured and either exposed to 2 Gy of gamma rays or not exposed to gamma rays (0 Gy). Chromosome spread assays were performed on irradiated ovaries after 1 and 8 h exposure time periods. **Aa**–**Fe**) Immunofluorescence with SYCP2 (green), RAD51 (red), and DMC1 (red) antibodies in wild-type (**Aa**–**Ce**) and *Hormad1*$^{-/-}$ zygotene oocytes (**Da**–**Fe**). DNA was stained with 4′,6-diamidino-2-phenylindole (DAPI, blue). Original magnification ×100. **G**) Graphic representation of DMC1 foci from 50 meiocytes at different exposure time points for specific genotypes. **H**) Graphic representation of RAD51 foci from 50 meiocytes at different exposure time points for specific genotypes. Error bars represent the SEM. Student *t*-test was used to calculate *P*-values (*$P < 0.05$).

after irradiation, and the increase persisted after 8 h (Fig. 3, Ac, Bc, Cc, and G). However, irradiation of *Hormad1*$^{-/-}$ zygotene oocytes did not significantly affect DMC1 foci formation (Fig. 3, Dc, Ec, Fc, and G). We also assessed RAD51 foci formation. Unlike DMC1, that is germ cell specific, RAD51 is ubiquitously expressed, involved in mitosis and meiosis, and is also important in DSB repair and inter-homologue recombination. The irradiated wild-type zygotene oocytes showed a 42.8% increase in the number of RAD51 foci (Fig. 3, Ad, Bd, and H). The irradiated *Hormad1*$^{-/-}$ zygotene oocytes also showed a 44% increase in the number of RAD51 foci (Fig. 3, Dd, Ed, and H). Eight hours after irradiation or sham treatment, the number of RAD51 foci was reduced to the level of nonirradiated wild-type and *Hormad1*$^{-/-}$ zygotene oocytes (Fig. 3, Cd, Fd, and H). These data are consistent with the interpretation that *Hormad1* deficiency interferes with DMC1 binding to DSB sites and that DSB repair may be accomplished in part by DMC1-independent DSB repair pathways.

### Hormad1 *Deficiency Rescues Oocyte Loss in* Dmc1$^{-/-}$ *Ovaries*

The above-described experiments are consistent with the interpretation that HORMAD1 inhibits DMC1-independent DSB repair pathways and that HORMAD1 deficiency allows DMC1-independent DSB repair to proceed. We therefore examined whether *Hormad1* deficiency can rescue accelerated loss of oocytes observed in the *Dmc1*$^{-/-}$ ovaries. DMC1-dependent interhomologue recombination is important in oocyte survival [2, 3, 13, 16, 38]. *Dmc1* deficiency leads to the accumulation of the extensively resected DSBs and massive oocyte loss shortly after birth [2]. We hypothesized that *Hormad1* deficiency would rescue *Dmc1*$^{-/-}$ oocyte loss, in part, by derepressing DMC1-independent DSB repair pathways. We crossed *Hormad1*$^{-/-}$ mice with *Dmc1*$^{-/-}$ mice to generate double knockouts. We examined the ovarian histology in wild-type, *Dmc1*$^{-/-}$, *Hormad1*$^{-/-}$, and *Dmc1*$^{-/-}$*Hormad1*$^{-/-}$ double-knockout mice. Three-day-old wild-type postnatal ovaries contain oocytes in germ cell clusters as well as primordial and some primary follicles. Histomorphometric assessment of the wild-type and *Hormad1*$^{-/-}$ 3-day-old postnatal ovaries showed 1147.4 ± 108.6 primordial and 68.5 ± 25.4 primary follicles in the wild-type mice (n = 5), 1184.6 ± 236.1 primary and 78.0 ± 33.4 primordial in the *Hormad1*$^{-/-}$ mice (n = 5), and 1317.8 ± 97.8 primary and 68.4 ± 19.2 primordial follicles in the *Dmc1*$^{-/-}$*Hormad1*$^{-/-}$ double-knockout mice (n = 3) (Fig. 4, A, B, D, and E). The numbers of primordial and primary follicles in wild-type, *Hormad1*$^{-/-}$, and *Dmc1*$^{-/-}$*Hormad1*$^{-/-}$ double-knockout ovaries at Postnatal Day 3 was not statistically significant. In contrast, very few primordial follicles were present in *Dmc1*$^{-/-}$ single-knockout ovaries (Fig. 4, C and E). At Postnatal Day 20, 677.0 ± 96.4, 677.1 ± 122.9, and 878.4 ± 300.7 primordial follicles; 60.8 ± 14.7, 40.6 ± 8.3, and 68.2 ± 8.1 primary follicles; 66.8 ± 17.1, 37.6 ± 10.6, and 88.6 ± 7.3 secondary follicles; and 54.2 ± 9.2, 44.0 ± 20.1, and 77.0 ± 20.3 preantral follicles were counted in wild-type (n = 5), *Hormad1*$^{-/-}$ (n = 5), and *Dmc1*$^{-/-}$*Hormad1*$^{-/-}$ (n = 3) ovaries, respectively (Fig. 4, F and H–J). The numbers of primordial and primary follicles in wild-type, *Hormad1*$^{-/-}$, and *Dmc1*$^{-/-}$*Hormad1*$^{-/-}$ ovaries at Postnatal Day 20 did not differ significantly (Fig. 4J). In contrast, almost no follicles remained in *Dmc1*$^{-/-}$ ovaries, as previously reported [2, 3] (Fig. 4G). Moreover, the 6-mo-old *Dmc1*$^{-/-}$*Hormad1*$^{-/-}$ ovaries were indistinguishable from the wild-type and *Hormad1*$^{-/-}$ ovaries, whereas no oocytes were detectable in *Dmc1*$^{-/-}$ ovaries (data not shown). Our data show that *Hormad1* deficiency rescued oocyte loss observed in DMC1-deficient mice. We also checked DSB formation in wild-type, *Dmc1*$^{-/-}$, *Hormad1*$^{-/-}$, and *Dmc1*$^{-/-}$*Hormad1*$^{-/-}$ zygotene oocytes using γH2AX antibody (Fig. 5, A–D). As expected, no significant difference was found in *Dmc1*$^{-/-}$ as compared to wild-type oocytes, but *Hormad1*$^{-/-}$ and *Dmc1*$^{-/-}$ *Hormad1*$^{-/-}$ oocytes showed a 50% reduced γH2AX signal compared to the wild-type zygonema (Fig. 5E). These results are consistent with our interpretation that HORMAD1 represses *Dmc1*-independent repair pathways and that HORMAD1 deficiency allows DMC1-independent pathways to operate and repair DSBs.

### Hormad1 *Deficiency Does Not Rescue Oocyte Loss in* Atm$^{-/-}$ *Ovaries*

We also examined the effects of *Hormad1* deficiency in *Atm* knockout mice. ATM is a serine/threonine-specific protein kinase that has been associated with cell-cycle regulation, apoptosis, and response to DNA damage repair [15, 29, 39, 40]. Recent data support a role for ATM in DSB formation during meiosis I [12]. ATM appears to control SPO11 activity via a negative-feedback loop in which ATM activation by DSBs suppress further DSB formation [12]. We showed previously that ATM kinase activation lies downstream of HORMAD1 [9]. We therefore hypothesized that ATM deficiency would stimulate a dramatic increase in SPO11 activity and a concomitant increase in DSB formation, which *Hormad1* deficiency will not rescue. Histomorphometric assessment at Postnatal Day 3 revealed only 10.6 ± 10.8 primordial follicles in the *Atm*$^{-/-}$ and 24.8 ± 17.1 (n = 3) in *Atm*$^{-/-}$*Hormad1*$^{-/-}$ mice as compared to more than 1,000 primordial follicles in the corresponding wild-type or *Hormad1*$^{-/-}$ mice (Figs. 4, A and C, and 6, A–C). We examined synaptonemal complex formation and DSBs in E16.5 wild-type, *Atm*$^{-/-}$, *Hormad1*$^{-/-}$, and *Atm*$^{-/-}$*Hormad1*$^{-/-}$ double-knockout oocytes using SYCP2 and γH2AX antibodies. *Atm*$^{-/-}$ zygonema showed a 37.4% increase in γH2AX intensity as compared with wild-type zygonema, whereas *Hormad1*$^{-/-}$ and *Atm*$^{-/-}$*Hormad1*$^{-/-}$ zygonema showed a 57.8% and 22.1% decrease, respectively, compared to wild-type zygonema (Fig. 6, D–G and L). However, *Atm*$^{-/-}$ *Hormad1*$^{-/-}$ zygonema oocytes had a significantly greater number of DSBs than *Hormad1*$^{-/-}$ single-knockout oocytes (Fig, 6, F and G). We also examined the zygopachynema in E16.5 wild-type, *Atm*$^{-/-}$, *Hormad1*$^{-/-}$, and *Atm*$^{-/-}$*Hormad1*$^{-/-}$ mice. *Atm*$^{-/-}$ and *Atm*$^{-/-}$*Hormad1*$^{-/-}$ zygopachynema showed a 102.7% and 76.5% increase, respectively, in γH2AX intensity ($P < 0.01$), whereas *Hormad1*$^{-/-}$ zygopachynema showed a 26.6% decrease, compared to wild-type zygonema ($P < 0.05$) (Fig. 6, H–L). Our data as well as those of others [9, 17, 19] are consistent with *Atm* deficiency causing an increase in the number of meiotic DSBs. Moreover, these results suggest that ATM is in part necessary for the DMC1-independent sister chromatid repair operating in *Hormad1*-deficient oocytes, because *Hormad1* deficiency was unable to decrease the formation of γH2AX foci.

## DISCUSSION

Many meiosis-specific components of the synaptonemal complex are critical in early folliculogenesis. For example, mutations in *Atm1, Dmc1*, *Sycp1*, *Sycp2*, and *Sycp3* accelerate oocyte loss [2–7, 29]. Perinatal germ cell loss in *Hormad1*-deficient mice does not differ significantly from that in wild-

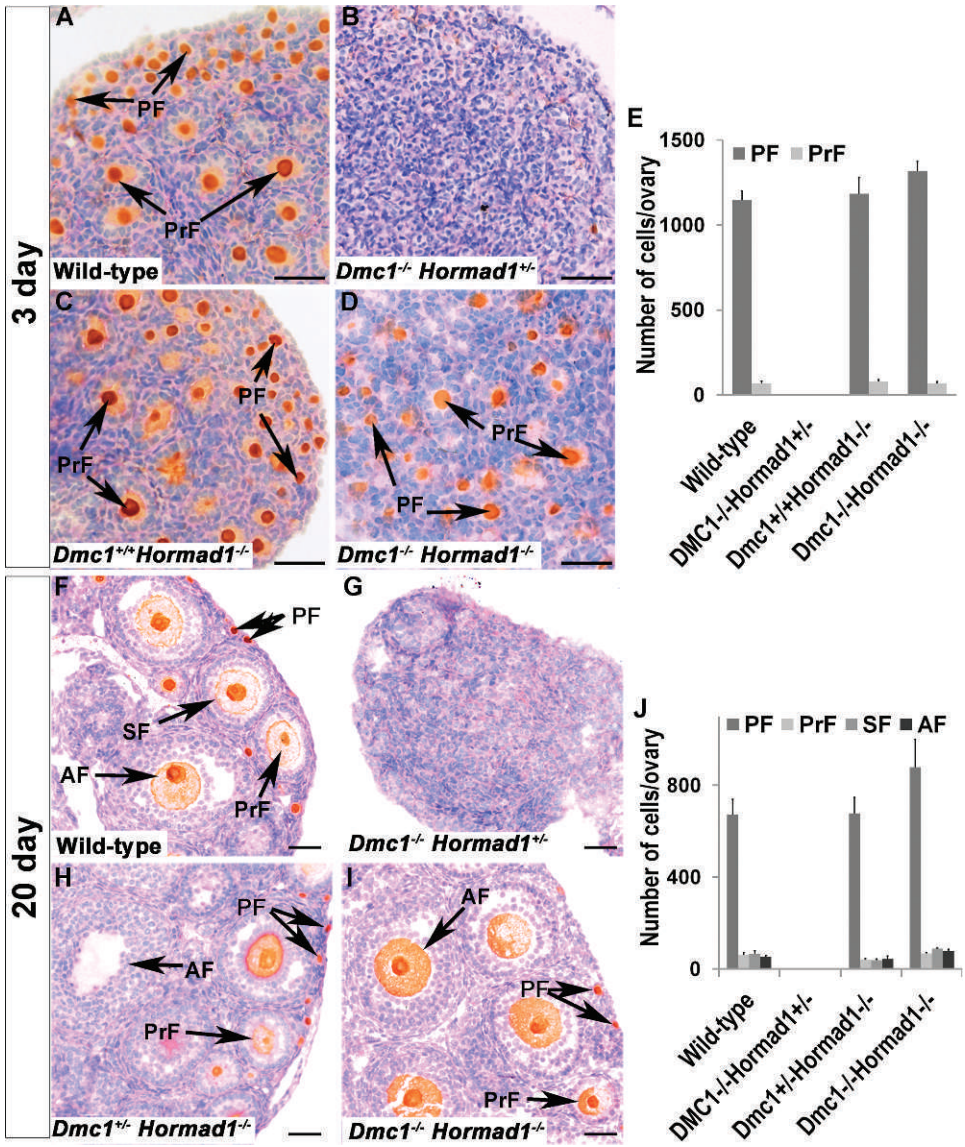


FIG. 4. *Hormad1* deficiency rescues oocyte survival in *Dmc1*$^{-/-}$ ovaries. NOBOX (postnatal oocyte-specific marker [8]) was used to detect oocytes by immunohistochemistry of ovaries from 3- and 20-day-old mice. Oocytes in primordial follicle (PF) and primary follicle (PrF) stages are shown in 3-day-old wild-type (**A**), *Hormad1*$^{-/-}$ (**C**), and *Dmc1*$^{-/-}$*Hormad1*$^{-/-}$ (**D**) ovaries. No PF follicles are visible in 3-day-old *Dmc1*$^{-/-}$*Hormad1*$^{+/-}$ ovaries (**B**). Oocytes in PF, PrF, secondary follicle (SF), and antral follicle (AF) stages are shown in 20-day-old wild-type (**F**), *Hormad1*$^{-/-}$ (**H**), and *Dmc1*$^{-/-}$*Hormad1*$^{-/-}$ (**I**) ovaries. No follicles were visible in 20-day old *Dmc1*$^{-/-}$ ovaries (**G**). There were no statistically significant differences between the wild-type, *Hormad1*$^{-/-}$, and *Dmc*$^{-/-}$*Hormad1*$^{-/-}$ double-knockout oocyte numbers at various follicle stages (**E** and **J**). Error bars represent the SEM. Bar = 50 μm.

type mice [9, 19, 21], despite formation of asynaptic oocytes. These findings as well as the absence of pachynema in *Hormad1*$^{-/-}$ meiocytes strongly support the argument that HORMAD1 is an important checkpoint protein essential for pachynema formation and elimination of asynaptic oocytes. HORMAD1 does this surveillance in part via DSB-independent pathways, because *Hormad1* deficiency can rescue *Spo11* mutants [19, 21]. *Spo11* mutants do not form DSBs, hence other mechanisms that trigger oocyte death must be involved [14].

The role of *Hormad1* in DSB repair and its role in oocyte survival have not been examined to date. Based on its HORMA domain and knockout phenotype in mice, HORMAD1 is the mammalian homologue to yeast Hop1. Hop1 in yeast has been implicated in facilitating interhomologue DSB repair and in repressing DMC1-independent intersister chromatid repair pathways [41, 42]. We therefore examined whether HORMAD1 actions in the mammalian system overlap what has been extensively studied with Hop1 in yeast. Our experimental findings are consistent with HORMAD1 playing a role similar to that of Hop1. First, our irradiation experiments show that gamma ray-induced DSBs persist over time in wild-type meiocytes but are significantly reduced in *Hormad1*$^{-/-}$ meiocytes. Moreover, *Hormad1* deficiency rescues *Dmc1* knockouts, and these double knockouts show normal folliculogenesis and ovarian development. DSBs in the *Dmc1*$^{-/-}$ *Hormad1*$^{-/-}$ mice are also significantly reduced as compared to the *Dmc1*$^{-/-}$ mice. MLH1, a protein that forms foci in later stages of recombination, is required for the formation of most of the crossovers (chiasmata) observed in mice and therefore is an excellent marker for meiotic crossovers [33, 43, 44]. The number of MLH1 foci in the *Hormad1*$^{-/-}$ oocytes was significantly reduced as compared to the wild-type oocytes [9, 19]. The lack of MLH1 foci (crossover markers) in

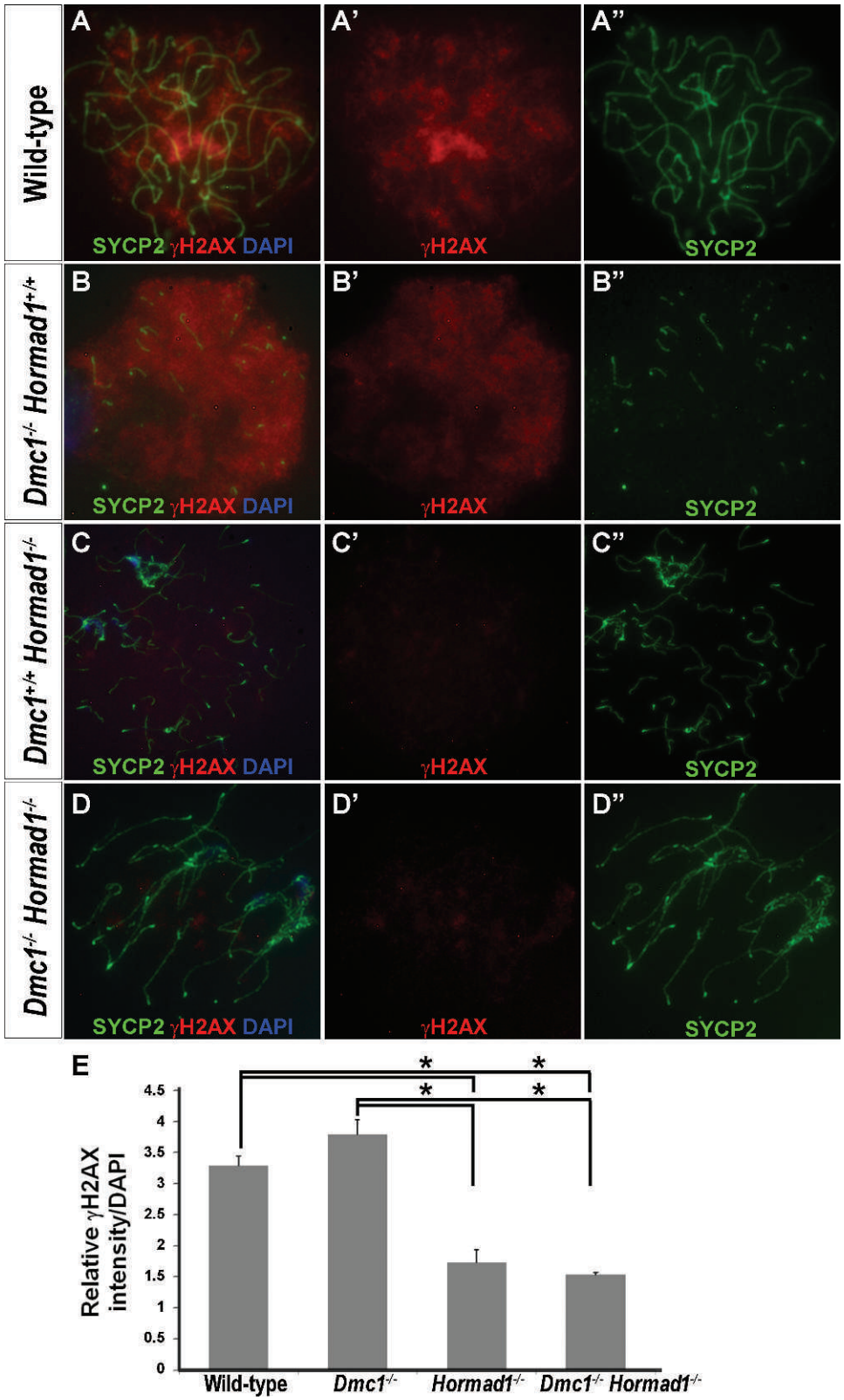


FIG. 5. *Hormad1* deficiency activates DMC1-independent DSB repair. DSB formation in *Dmc1*$^{-/-}$, *Hormad1*$^{-/-}$, and *Dmc1*$^{-/-}$*Hormad1*$^{-/-}$ zygonema as compared to the wild-type. Immunofluorescence with γH2AX (red; **A**′–**D**′) and SYCP2 (green, **A**″–**D**″) antibodies in wild-type (**A**), *Dmc1*$^{-/-}$ (**B**), *Hormad1*$^{-/-}$ (**C**), and *Dmc1*$^{-/-}$*Hormad1*$^{-/-}$ (**D**) zygonema. DNA was stained with 4′,6-diamidino-2-phenylindole (DAPI; blue). Original magnification ×100. **E**) Relative intensity of γH2AX was determined on 50 oocytes for various genotypes (**A**–**D**). The intensity of γH2AX was normalized against DAPI. Error bars represent the SEM. Student *t*-test was used to calculate *P*-values (*$P < 0.01$).

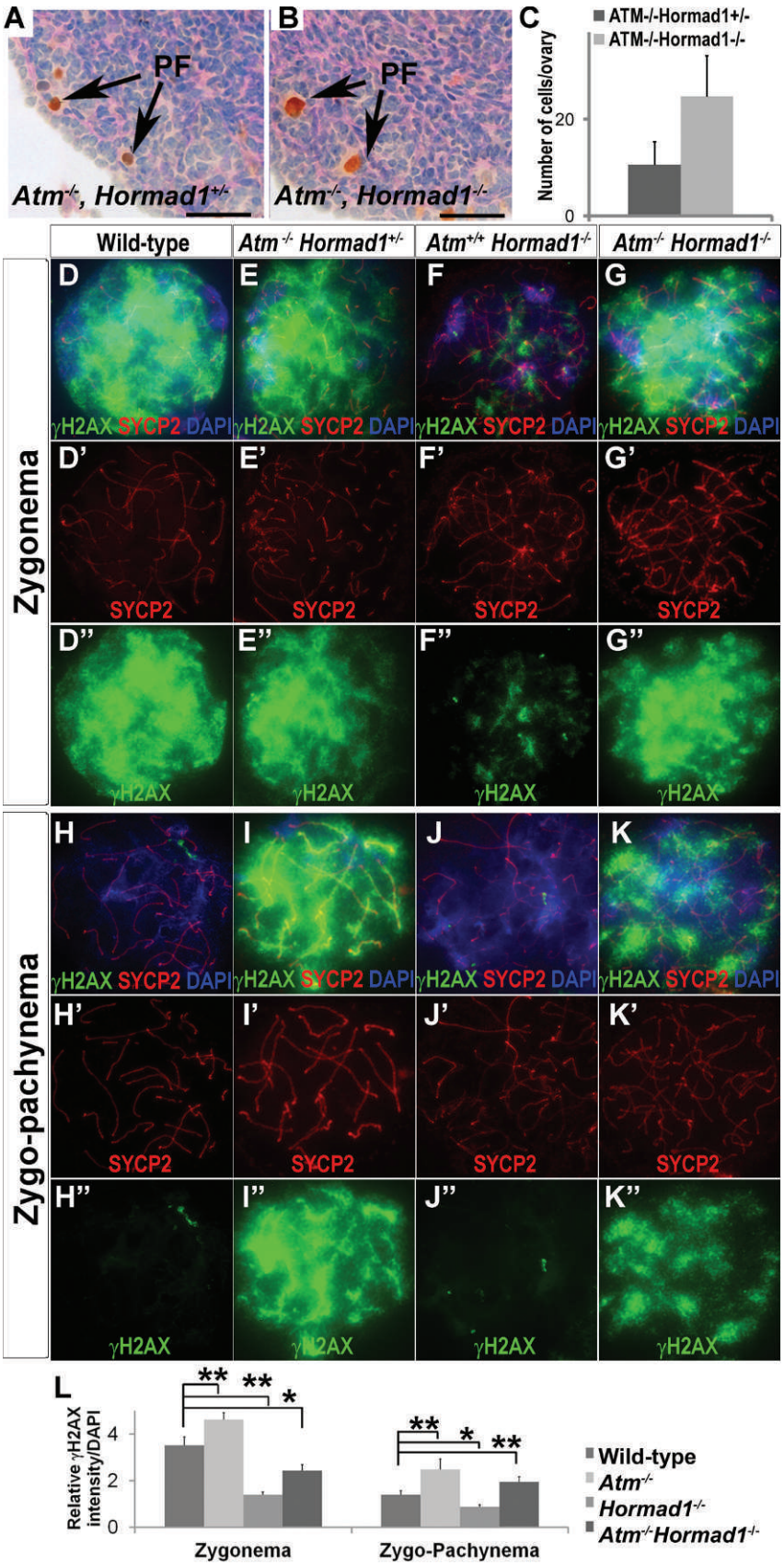


FIG. 6. *Hormad1* deficiency cannot rescue $Atm^{-/-}$ mice. We generated $Atm^{-/-}Hormad1^{-/-}$ double-knockout mice to assess effects of double deficiency on ovarian development and DSB formation. NOBOX was used to detect oocytes by immunohistochemistry on ovaries from 3-day-old mice. Only a few primordial follicles (PF) were visible in 3-day-old $Atm^{-/-}$ and $Atm^{-/-}Hormad1^{-/-}$ ovaries ($P > 0.05$) (**A**–**C**). These results indicate that *Hormad1* deficiency cannot rescue $Atm^{-/-}$ ovarian phenotype. Bar = 50 μm (**A** and **B**). **D**–**K**) Immunofluorescence with γH2AX (red) and SYCP2 (green) antibodies in wild-type (**D** and **H**), $Atm^{-/-}$ (**E** and **I**), $Hormad1^{-/-}$ (**F** and **J**), and $Atm1^{-/-}Hormad1^{-/-}$ (**G** and **K**) ovaries. DNA was stained with

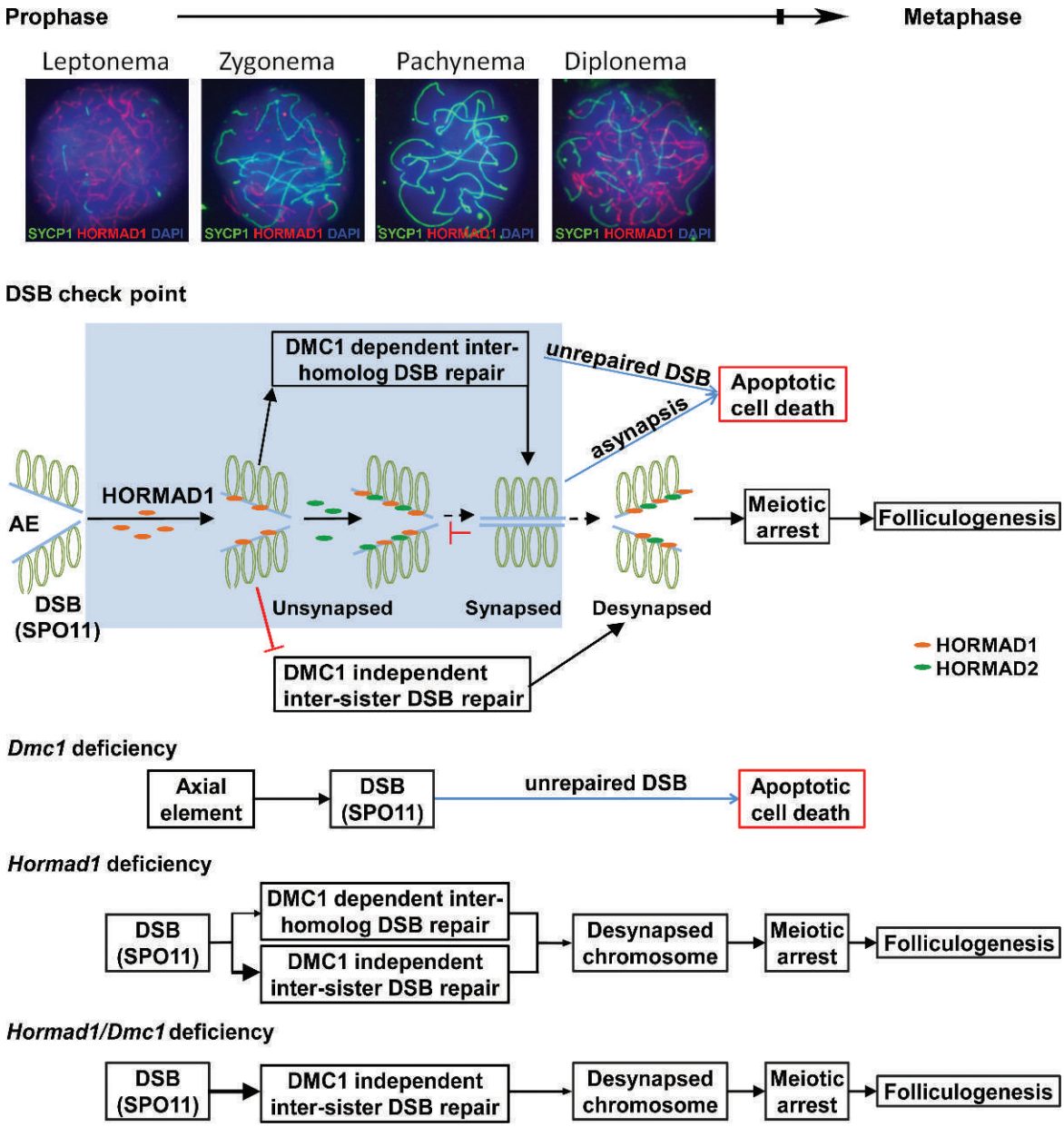


FIG. 7. Summary of HORMAD1 functions as a major checkpoint in female meiosis. In early prophase, axial element formation causes DSBs by SPO11 and phosphorylated HORMAD1 localizes on unsynapsed chromosomes (leptonema and zygonema). HORMAD1 stimulates synaptonemal complex formation and DMC1-dependent interhomologue DSB repair [9, 17, 19, 21]. Sequential HORMAD1 and HORMAD2 binding to unsynapsed chromosome lead to meiotic silencing of unsynapsed chromosomes [46, 47] and synaptonemal complex formation. Synaptonemal complex formation leads to HORMAD1 depletion from the synapsed chromosomes (pachynema) [9, 17, 19, 21]. HORMAD1 and HORMAD2 were localized at the desynapsed axes in diplonema. After that, oocytes arrest in dictyate stage of meiosis I until ovulation in puberty. HORMAD1 blocks the DMC1-independent intersister DSB repair and consequently activates DMC1-dependent interhomologue DSB repair. Unrepaired DSBs associate with germ cell death, and HORMAD1 deficiency activates DMC1-independent intersister DSB repair, bypassing the DSB check point and ensuring oocyte survival [2–4, 13]. Original magnification ×100.

*Hormad1*$^{-/-}$ oocytes also supports the interpretation that *Hormad1* deficiency leads to DMC1-independent intersister DSB repair and noncrossover. The above-mentioned observations are all consistent with the interpretation that HORMAD1 blocks DMC1-independent DSB repair pathways and that in the absence of HORMAD1, DMC1 independent mechanisms activate intersister chromatid repair.

Our data also show that *Hormad1* deficiency cannot rescue the *Atm* ovarian phenotype. *Atm*$^{-/-}$ embryonic ovaries enter leptonema, zygonema, and pachynema, but oocytes begin to degenerate late in embryogenesis before dictyate arrest so that by 11 days, few oocytes remain [2–4]. The loss of oocytes in *Atm*$^{-/-}$ ovaries is likely due to the meiosis arrest at the zygotene/pachytene stage of prophase I, as a result of abnormal

4′,6-diamidino-2-phenylindole (DAPI; blue). **L**) Relative intensity of γH2AX normalized against DAPI was calculated and plotted in a graph form for indicated genotypes and meiotic stages (**D**–**K**). Original magnification ×100. Error bars represent the SEM. Student *t*-test was used to calculate *P*-values (* $P < 0.05$, ** $P < 0.01$).

chromosomal synapsis and subsequent chromosome fragmentation [4]. ATM does not appear to affect HORMAD1, because HORMAD1 phosphorylation and localization is normal in *Atm*$^{-/-}$ gonads [9]. Moreover, HORMAD1 deficiency does not abrogate ATM autophosphorylation (phospho-S1981) in the ovary (data not shown). Why is it that *Hormad1* deficiency cannot rescue *Atm*$^{-/-}$ whereas *Spo11* deficiency can? ATM inactivation leads to a great increase in DSBs, with 10-fold elevation in steady-state levels of SPO11-oligonucleotide complexes [12]. Whereas in *Spo11* mutants DSBs do not form, in *Atm* mutants DSBs are produced at a higher rate [12]. Our data as well as previously reported *Hormad1*/*Spo11* double-knockout rescue results [19, 21] are consistent with HORMAD1 modulating both DNA damage-dependent and DNA damage-independent responses. HORMAD1 clearly is a major checkpoint protein in oocyte meiosis and coordinates both checkpoint signaling and chromosome behavior (Fig. 7).

Phosphorylation of HORMAD1 and HORMAD2 correlates with their localization to unsynapsed chromosome axes but not to synapsed regions [20]. Phosphorylation is reduced in the absence of initiation of meiotic recombination, and these studies suggest that modifications of chromosome axis components signal recombination, checkpoint control, transcription, and synapsis regulation [20]. These findings are in line with recent experiments that show partial rescue of the *Dmc1*$^{-/-}$ phenotype by the synaptonemal complex protein SYCP3 [45].

Another germ cell-specific HORMA domain protein, HORMAD2, was recently identified in mammals [17]. HORMAD2 localizes to the synaptonemal complex after HORMAD1 binding and is involved in the meiotic silencing mechanism at the unsynapsed chromatin [46, 47]. HORMAD1 and HORMAD2 do not appear to interact physically [20]. Interestingly, HORMAD2 has no effect on female fertility, oocyte numbers, and RAD51, DMC1, and MLH1 foci in the knockout [46]. HORMAD2 cannot rescue oocyte loss in *Dmc1*$^{-/-}$ ovaries; however, *Hormad2* deficiency can rescue oocyte loss in *Spo11*$^{-/-}$ ovaries [46, 47]. HORMAD1, on the other hand, can rescue both *Spo11*$^{-/-}$ [19] and *Dmc1*$^{-/-}$ phenotypes (Fig. 4). Therefore, HORMAD1 has a dominant function in the female DSB repair pathway (Fig. 7) as well as in the female asynapsis surveillance. It has been proposed that HORMAD2 is important for the asynapsis surveillance in females based on its rescue of *Spo11* as well as the barely significant increase in univalent-containing metaphase I oocytes [46]. This is indeed surprising, because HORMAD2 is functionally neutral in the female, at least based on the reported normal fertility and ovarian development phenotype. It would be interesting to assess whether *Hormad2*$^{-/-}$ ovaries are more susceptible to environmental stress, such as chemotherapy and radiation.

Although HORMAD1 plays a critical role in meiotic surveillance, HORMAD1 deficiency does not decelerate the natural loss of oocytes that occurs as the germ cell clusters break down to form primordial follicles. The loss of oocytes at that stage is enormous—more than 50% are lost [1]—and likely determines individual endowment and reproductive life span. If HORMAD1 plays a major role in meiotic surveillance and asynapsis as well as unrepaired DNA damage are the cause of perinatal oocyte atresia, we would expect a higher number of primordial follicles in *Hormad1*$^{-/-}$ animals. Although a trend to a greater number of primordial follicles was observed in *Hormad1*$^{-/-}$ ovaries compared to wild-type ovaries (Supplemental Fig. S1), the trend was not statistically significant. These results suggest that meiotic errors per se may not be the major determinant of oocyte loss during formation of the primordial follicle and that other pathways are involved.

## REFERENCES


1. Pepling ME, Spradling AC. Mouse ovarian germ cell cysts undergo programmed breakdown to form primordial follicles. Dev Biol 2001; 234: 339–351.
2. Pittman DL, Cobb J, Schimenti KJ, Wilson LA, Cooper DM, Brignull E, Handel MA, Schimenti JC. Meiotic prophase arrest with failure of chromosome synapsis in mice deficient for *Dmc1*, a germline-specific RecA homolog. Mol Cell 1998; 1:697–705.
3. Yoshida K, Kondoh G, Matsuda Y, Habu T, Nishimune Y, Morita T. The mouse *RecA*-like gene *Dmc1* is required for homologous chromosome synapsis during meiosis. Mol Cell 1998; 1:707–718.
4. Barlow C, Liyanage M, Moens PB, Tarsounas M, Nagashima K, Brown K, Rottinghaus S, Jackson SP, Tagle D, Ried T, Wynshaw-Boris A. Atm deficiency results in severe meiotic disruption as early as leptonema of prophase I. Development 1998; 125:4007–4017.
5. de Vries FA, de Boer E, van den Bosch M, Baarends WM, Ooms M, Yuan L, Liu JG, van Zeeland AA, Heyting C, Pastink A. Mouse *Sycp1* functions in synaptonemal complex assembly, meiotic recombination, and XY body formation. Genes Dev 2005; 19:1376–1389.
6. Yang F, De La Fuente R, Leu NA, Baumann C, McLaughlin KJ, Wang PJ. Mouse SYCP2 is required for synaptonemal complex assembly and chromosomal synapsis during male meiosis. J Cell Biol 2006; 173: 497–507.
7. Wang H, Hoog C. Structural damage to meiotic chromosomes impairs DNA recombination and checkpoint control in mammalian oocytes. J Cell Biol 2006; 173:485–495.
8. Rajkovic A, Pangas SA, Ballow D, Suzumori N, Matzuk MM. NOBOX deficiency disrupts early folliculogenesis and oocyte-specific gene expression. Science 2004; 305:1157–1159.
9. Shin YH, Choi Y, Erdin SU, Yatsenko SA, Kloc M, Yang F, Wang PJ, Meistrich ML, Rajkovic A. *Hormad1* mutation disrupts synaptonemal complex formation, recombination, and chromosome segregation in mammalian meiosis. PLoS Genet 2010; 6:e1001190.
10. Pangas SA, Choi Y, Ballow DJ, Zhao Y, Westphal H, Matzuk MM, Rajkovic A. Oogenesis requires germ cell-specific transcriptional regulators *Sohlh1* and *Lhx8*. Proc Natl Acad Sci U S A 2006; 103: 8090–8095.
11. Choi Y, Yuan D, Rajkovic A. Germ cell-specific transcriptional regulator *Sohlh2* is essential for early mouse folliculogenesis and oocyte-specific gene expression. Biol Reprod 2008; 79:1176–1182.
12. Lange J, Pan J, Cole F, Thelen MP, Jasin M, Keeney S. ATM controls meiotic double-strand-break formation. Nature 2011; 479:237–240.
13. Baudat F, Manova K, Yuen JP, Jasin M, Keeney S. Chromosome synapsis defects and sexually dimorphic meiotic progression in mice lacking Spo11. Mol Cell 2000; 6:989–998.
14. Di Giacomo M, Barchi M, Baudat F, Edelmann W, Keeney S, Jasin M. Distinct DNA-damage-dependent and -independent responses drive the loss of oocytes in recombination-defective mouse mutants. Proc Natl Acad Sci U S A 2005; 102:737–742.
15. Barchi M, Roig I, Di Giacomo M, de Rooij DG, Keeney S, Jasin M. ATM promotes the obligate XY crossover and both crossover control and chromosome axis integrity on autosomes. PLoS Genet 2008; 4:e1000076.
16. Romanienko PJ, Camerini-Otero RD. The mouse *Spo11* gene is required for meiotic chromosome synapsis. Mol Cell 2000; 6:975–987.
17. Wojtasz L, Daniel K, Roig I, Bolcun-Filas E, Xu H, Boonsanay V, Eckmann CR, Cooke HJ, Jasin M, Keeney S, McKay MJ, Toth A. Mouse HORMAD1 and HORMAD2, two conserved meiotic chromosomal proteins, are depleted from synapsed chromosome axes with the help of TRIP13 AAA-ATPase. PLoS Genet 2009; 5:e1000702.
18. Fukuda T, Daniel K, Wojtasz L, Toth A, Hoog C. A novel mammalian HORMA domain-containing protein, HORMAD1, preferentially associates with unsynapsed meiotic chromosomes. Exp Cell Res 2010; 316: 158–171.
19. Daniel K, Lange J, Hached K, Fu J, Anastassiadis K, Roig I, Cooke HJ, Stewart AF, Wassmann K, Jasin M, Keeney S, Toth A. Meiotic homologue alignment and its quality surveillance are controlled by mouse HORMAD1. Nat Cell Biol 2011; 13:599–610.
20. Fukuda T, Pratto F, Schimenti JC, Turner JM, Camerini-Otero RD, Hoog C. Phosphorylation of chromosome core components may serve as axis marks for the status of chromosomal events during mammalian meiosis. PLoS Genet 2012; 8:e1002485.
21. Kogo H, Tsutsumi M, Ohye T, Inagaki H, Abe T, Kurahashi H.

HORMAD1-dependent checkpoint/surveillance mechanism eliminates asynaptic oocytes. Genes Cells 2012; 17:439–454.
22. Aravind L, Koonin EV. The HORMA domain: a common structural denominator in mitotic checkpoints, chromosome synapsis and DNA repair. Trends Biochem Sci 1998; 23:284–286.
23. Hollingsworth NM, Goetsch L, Byers B. The *HOP1* gene encodes a meiosis-specific component of yeast chromosomes. Cell 1990; 61:73–84.
24. Smith AV, Roeder GS. The yeast Red1 protein localizes to the cores of meiotic chromosomes. J Cell Biol 1997; 136:957–967.
25. Couteau F, Nabeshima K, Villeneuve A, Zetka M. A component of *C. elegans* meiotic chromosome axes at the interface of homolog alignment, synapsis, nuclear reorganization, and recombination. Curr Biol 2004; 14: 585–592.
26. Zetka MC, Kawasaki I, Strome S, Muller F. Synapsis and chiasma formation in *Caenorhabditis elegans* require HIM-3, a meiotic chromosome core component that functions in chromosome segregation. Genes Dev 1999; 13:2258–2270.
27. Sanchez-Moran E, Santos JL, Jones GH, Franklin FC. ASY1 mediates AtDMC1-dependent interhomolog recombination during meiosis in *Arabidopsis*. Genes Dev 2007; 21:2220–2233.
28. Kironmai KM, Muniyappa K, Friedman DB, Hollingsworth NM, Byers B. DNA-binding activities of Hop1 protein, a synaptonemal complex component from *Saccharomyces cerevisiae*. Mol Cell Biol 1998; 18: 1424–1435.
29. Xu Y, Ashley T, Brainerd EE, Bronson RT, Meyn MS, Baltimore D. Targeted disruption of ATM leads to growth retardation, chromosomal fragmentation during meiosis, immune defects, and thymic lymphoma. Genes Dev 1996; 10:2411–2422.
30. Hama H, Kurokawa H, Kawano H, Ando R, Shimogori T, Noda H, Fukami K, Sakaue-Sawano A, Miyawaki A. Sca*l*e: a chemical approach for fluorescence imaging and reconstruction of transparent mouse brain. Nat Neurosci 2011; 14:1481–1488.
31. O'Brien MJ, Pendola JK, Eppig JJ. A revised protocol for in vitro development of mouse oocytes from primordial follicles dramatically improves their developmental competence. Biol Reprod 2003; 68: 1682–1686.
32. Tilly JL. Ovarian follicle counts—not as simple as 1, 2, 3. Reprod Biol Endocrinol 2003; 1:11.
33. Moens PB, Kolas NK, Tarsounas M, Marcon E, Cohen PE, Spyropoulos B. The time course and chromosomal localization of recombination-related proteins at meiosis in the mouse are compatible with models that can resolve the early DNA-DNA interactions without reciprocal recombination. J Cell Sci 2002; 115:1611–1622.
34. Buard J, Barthes P, Grey C, de Massy B. Distinct histone modifications define initiation and repair of meiotic recombination in the mouse. EMBO J 2009; 28:2616–2624.
35. Prieler S, Penkner A, Borde V, Klein F. The control of Spo11's interaction with meiotic recombination hotspots. Genes Dev 2005; 19:255–269.
36. Sedelnikova OA, Rogakou EP, Panyutin IG, Bonner WM. Quantitative detection of $^{125}$IdU-induced DNA double-strand breaks with gamma-H2AX antibody. Radiat Res 2002; 158:486–492.
37. Stewart RD. Two-lesion kinetic model of double-strand break rejoining and cell killing. Radiat Res 2001; 156:365–378.
38. Howard-Till RA, Lukaszewicz A, Loidl J. The recombinases Rad51 and Dmc1 play distinct roles in DNA break repair and recombination partner choice in the meiosis of *Tetrahymena*. PLoS Genet 2011; 7:e1001359.
39. Goodarzi AA, Block WD, Lees-Miller SP. The role of ATM and ATR in DNA damage-induced cell cycle control. Prog Cell Cycle Res 2003; 5: 393–411.
40. Moens PB, Tarsounas M, Morita T, Habu T, Rottinghaus ST, Freire R, Jackson SP, Barlow C, Wynshaw-Boris A. The association of ATR protein with mouse meiotic chromosome cores. Chromosoma 1999; 108:95–102.
41. Latypov V, Rothenberg M, Lorenz A, Octobre G, Csutak O, Lehmann E, Loidl J, Kohli J. Roles of Hop1 and Mek1 in meiotic chromosome pairing and recombination partner choice in *Schizosaccharomyces pombe*. Mol Cell Biol 2010; 30:1570–1581.
42. Carballo JA, Johnson AL, Sedgwick SG, Cha RS. Phosphorylation of the axial element protein Hop1 by Mec1/Tel1 ensures meiotic interhomolog recombination. Cell 2008; 132:758–770.
43. Edelmann W, Cohen PE, Kneitz B, Winand N, Lia M, Heyer J, Kolodner R, Pollard JW, Kucherlapati R. Mammalian MutS homologue 5 is required for chromosome pairing in meiosis. Nat Genet 1999; 21:123–127.
44. Anderson LK, Reeves A, Webb LM, Ashley T. Distribution of crossing over on mouse synaptonemal complexes using immunofluorescent localization of MLH1 protein. Genetics 1999; 151:1569–1579.
45. Li XC, Bolcun-Filas E, Schimenti JC. Genetic evidence that synaptonemal complex axial elements govern recombination pathway choice in mice. Genetics 2011; 189:71–82.
46. Wojtasz L, Cloutier JM, Baumann M, Daniel K, Varga J, Fu J, Anastassiadis K, Stewart AF, Remenyi A, Turner JM, Toth A. Meiotic DNA double-strand breaks and chromosome asynapsis in mice are monitored by distinct HORMAD2-independent and -dependent mechanisms. Genes Dev 2012; 26:958–973.
47. Kogo H, Tsutsumi M, Inagaki H, Ohye T, Kiyonari H, Kurahashi H. HORMAD2 is essential for synapsis surveillance during meiotic prophase via the recruitment of ATR activity. Genes Cells 2012; 17:897–912.